

Characterization of Self-Healing Fiber-Reinforced Polymer-Matrix Composite with Distributed Damage

Ever J. Barbero and Kevin J. Ford

Mechanical and Aerospace Engineering, West Virginia University, Morgantown, WV

Abstract

The objective of this manuscript is to describe experimental work that quantifies the damage and self-healing behavior of fiber-reinforced, polymer-matrix, laminated composites. The effects of damage and healing on stiffness and strength are described. While previous research looks at healing of macro-cracks, this work studies the healing of micro-cracks. Therefore, this work quantifies the effect of damage and self-healing within the context of continuum damage mechanics. This work also evaluates the effects of incorporating a self-healing system on the overall material properties of a laminate before and after the self-healing system is self-activated. Self-healing of glass fiber-reinforced epoxy laminates is accomplished by a dispersion of micro-capsules containing a healing agent and an encapsulated catalyst. The healing agent, dicyclopentadiene is encapsulated and then dispersed in the epoxy resin during hand lay-up. The catalyst capable of initiating a ROMP reaction with the DCPD is also encapsulated and dispersed in similar fashion. Continuum Damage Mechanics is used purposely to avoid having to investigate the micro-structural features of the complex composite/healing system but rather to assess the composite's performance using macroscopic features, i.e., reduced stiffness, which directly relates to structural performance as it is much easier to quantify experimentally.

Introduction

Composite materials are formed by the combination of two or more distinct materials to form a new material with enhanced properties¹. Recently, a number of self-healing systems have been proposed²⁻⁶. Of particular interest to us are self-healing polymers and composites. One system in particular incorporates the use of urea-formaldehyde micro-capsules filled with dicyclopentadiene (DCPD) and Ruthenium catalyst⁷⁻¹⁰. Micro-capsules and catalyst are uniformly dispersed in the matrix material. The micro-capsules are ruptured by growing micro-cracks in the composite. While prior literature has shown that macro-cracks are able to cause the release the healing agent¹¹⁻¹⁴, the present work shows that distributed damage in the form of micro-cracks also initiates the release of healing agent. Once ruptured, the micro-capsules release the DCPD, which travels through capillary action into the propagated crack and comes into contact with the catalyst¹⁵. The chemical reaction creates a living polymer¹⁶⁻¹⁸ that fills the void made by the micro-crack, thus healing the composite. Prior research deals with experimental study of fracture toughness of double cantilever beam, tapered cantilever beam, and compact tension specimens^{7,8,11,12} where an induced macro-crack is then healed. Specimens with induced macro-fractures have been used to show as much as 75% fracture toughness recovery^{7,8}. The present work considers healing of micro-cracks and quantifies the effects of incorporating a self-healing system on the overall material properties of a laminate, before and after the self-healing system is self-activated. Fabrication of a composite with both micro-capsules and healing agent dispersed in the intra-laminar region, and subsequent testing to demonstrate autonomic healing is accomplished.

The self-healing system uses the ROMP reaction of dicyclopentadiene¹⁷ with Grubbs' Ru catalyst¹⁸, which does not require precise stoichiometry and it can be triggered at low concentration¹¹. Several variations of the encapsulation process of DCPD have been discussed in the literature¹⁹⁻²⁸. Agitation rate in the range 200-2000 rpm controls the diameter of the microcapsule^{23,28}. Typical fill content of the micro-capsules is 83-92 %wt DCPD and 6-12 %wt urea-formaldehyde, 2-5% water²³. Typically the average fill content of the micro-capsules decreases by 2.3 %wt after 30 days in ambient conditions²³ and thus, shelf life is a concern. The strength and permeability of the micro-capsules is controlled by the shell wall thickness, typically in the 0.2-1.3 micron range. It is important that the shell wall is strong enough to keep the capsule from breaking during the lay-up process, yet still rupture when the crack reaches the microcapsule.

In^{11,29}, the crack-healing efficiency is defined as the % recovery of fracture toughness measured by tapered double-cantilever beam (TDCB). The specimens were allowed to heal for 48 hr before they were retested. The healing efficiency increases and the gel time decreases exponentially as the concentration of the catalyst increases. Catalyst concentrations in the range 2-40 g/Liter of catalyst to DCPD ratio were studied¹¹. Concentrations of 0-25 wt% of 180 micron diameter micro-capsules were used in samples that were fractured; then healed manually¹¹. The virgin fracture toughness of the material increases as the concentration of micro-capsules increases the range 0-25% weight of micro-capsules to Epoxy (EPON 828) and 12 pph DETA curing agent. Near perfect healing is obtained at 25% wt.

Grubbs' catalyst retains its activity when mixed with the EPON® 828/DETA system during cure. However, when

mixed with the DETA curing agent alone the catalyst experiences rapid deactivation¹¹. Catalyst particle sizes in the range 180-355 microns produce the highest healing efficiency out of a range 75-1000 micron studied¹¹. The virgin fracture toughness decreases and the healing efficiency increases as the concentration of the catalyst increases from 0-4 %wt of resin¹¹. This is due to the toughening effect of the foreign particles in the neat Epoxy. Maximum toughness reported in the literature may reach 127 % of the neat epoxy toughness. Smaller micro-capsules yield more toughening even at lower concentrations³⁰.

Larger micro-capsules yield greater efficiency. While using 2.5 %wt catalyst and 10 %wt micro-capsules with sizes in the 180-460 micron range, the 460 micron micro-capsules yield the greatest healing efficiency¹¹. The time for the reaction of Grubbs' catalyst and the DCPD healing agent also plays an important role in the healing efficiency of the specimen. Using 5-10 %wt of 180 microns diameter micro-capsules and 2.5 wt% catalyst, significant healing efficiencies develop after 25 min and steady-state values are reached after 10 hr¹¹.

Delamination healing between layers of woven composites is reported in¹², where the catalyzed healing agent was manually injected into the delamination region. Alternatively, un-catalyzed healing agent was injected into the delamination region of specimens that had only catalyst embedded.

The rate of in-situ polymerization for self-activated materials must be fast to prevent diffusion of the monomer into the matrix¹⁶. Since the healing system is a living polymerization, repeated healing can occur¹⁶. The healing efficiency increases with the time the specimen is allowed to heal until a maximum efficiency is reached at 48 Hr¹⁵.

Since the catalyst does not disperse well in the epoxy matrix and Diethylenetriamine (DETA) severely degrades the catalyst as the epoxy initially cures, the catalyst was encapsulated in paraffin wax³¹. DCB fracture toughness after healing with encapsulated catalyst loading in the range 0-1.25 %wt increases with catalyst loading up to 0.75 %wt, reaching a healing efficiency of 93%³¹.

Other healing processes such as geological rock densification³², self-healing healing of concrete^{33,34}, and self-healing healing of ceramic materials^{35,36} have been discussed in the literature. Some models for bone remodeling or wounded skin regeneration have been developed for relatively simple cases³⁷⁻³⁹. A constitutive model for compaction of crushed rock salt has been proposed in the thermodynamic framework³².

Barbero et al.⁴⁰ developed a Continuous Damage and Healing Mechanics (CDHM) model to predict the effects of damage and subsequent self-healing as a function of load history. The damage portion of the model has been extensively identified and verified with data available in the literature⁴¹⁻⁴⁶. The self-healing portion of the models could not be identified nor verified until now because lack of experimental data for laminates undergoing distributed damage (e.g., micro-cracking). Prior data exists only for fracture toughness recovery due to healing of macro-cracks. There-

fore, the objective of this manuscript is to describe experimental work that quantifies the damage and self-healing behavior of fiber-reinforced, polymer-matrix, laminated composites subjected to micro-crack damage. The effects of damage, healing, damage hardening, and hardening recovery upon healing, are described. This work also evaluates the effects of incorporating a self-healing system on the overall material properties of a laminate before and after the self-healing system is self-activated.

Materials and Methods

Ethylene maleic anhydride (EMA) copolymer was obtained from Zeeland Chemicals. Dicyclopentadiene (DCPD), urea, ammonium chloride, formaldehyde, and sodium hydroxide were purchased from Fisher Scientific. Resorcinol, hydrochloric acid, and 1-octanol were purchased from J.T. Baker. K-type thermocouples and thermocouple reader were purchased from OMEGA. A Eurostar power control-visc digital mixer was purchased from IKA Works, INC. A three-bladed, 63.5mm diameter low-shear mixing impeller was purchased from Cole Parmer. All solvents and substance used for preparation of EMA solution, acid and base solutions and 1-octanol were of analytical grade. Bis(tricyclohexylphosphine)benzylidene ruthenium (IV) dichloride (Grubbs' Ru catalyst) was purchased from Materia. A Gilson Performer III sieve shaker and sieves were purchased from Gilson Company, Inc. Neutral activated aluminum oxide and paraffin wax was purchased from Sigma Aldrich.

Samples were fabricated by hand lay-up and vacuum bagging of fiberglass/Epoxy with 52% fiber volume fraction for all systems. The addition of micro-capsules reduces the matrix volume fraction only. The reinforcement contains 90% of the fibers in the longitudinal direction and 10% in the transverse direction in a non-woven, non-stitched system, which is held together by a binding agent when dry. Various laminate stacking sequences (LSS) were fabricated including unidirectional $[0]_T$, cross-ply $[0]90_s$, and $[(0/90)]_n/45/-45_s$, where n is the number of (0/90) groups, including quasi-isotropic $[0/90/45/-45]_s$. Unidirectional $[0]_T$ were used to identify the model parameters (Tables 1 and 2). All other laminate stacking sequences (LSS) were used to verify the model prediction. The model is reported in^{40,47}.

Samples were fabricated with and without the self healing system. Those with self healing contained encapsulated DCPD at 20%wt of Epoxy and wax-encapsulated catalyst at 1.5 %wt of Epoxy. Vacuum bagging technique is used to consolidate the samples, which are cured at room temperature for 24 Hr. Tensile ASTM D3039⁴⁸, compressive SACMA-SRM-1R-94⁴⁹, and shear ASTM D5379⁵⁰ specimens were cut from these samples.

In order to observe the damage effects uncoupled from the healing effects, three types of tests were conducted. Damage tests of unidirectional samples having no self-healing were conducted to obtain baseline properties. Damage tests of unidirectional samples with self-healing system were conducted within a short period of time (two minutes or less at a loading rate of 0.05 in/min) without allow-

Table 1. Material properties of unidirectional composite without self-healing system (see Nomenclature).

Material Property	Value	Number of Specimens	Standard Deviation	Coefficient of Variation (%)
E_1 (MPa)	34784	5	2185.89	6.28
E_2 (MPa)	13469	3	587.32	4.36
ν_{12}	0.255	5	0.032	12.61
ν_{13}	0.255	5	0.032	12.61
G_{12} (MPa)	3043	5	439.74	14.45
F_{1r} (MPa)	592.3	5	29.32	4.95
F_{1c} (MPa)	459.1	5	43.66	9.51
F_{2r} (MPa)	68.86	3	9.17	13.32
F_{2c} (MPa)	109.5	6	9.25	8.45
F_6 (MPa)	49.87	5	3.39	6.79

Table 2. Virgin material properties of samples containing the self-healing system.

Material Property	Value	Number of Specimens	Standard Deviation	Coefficient of Variation (%)	%reduction w.r.t Table 1
E_1 (MPa)	30571	7	4185	13.7	-12
E_2 (MPa)	8699	7	829	9.5	-35
ν_{12}	0.251	6	0.035	14.1	-1.5
G_{12} (MPa)	2547	5	207	8.2	-6
F_{1r} (MPa)	397	7	66	16.6	-33
F_{1c} (MPa)	232	5	59	25.5	-52
F_{2r} (MPa)	45	7	10	23.5	-34
F_{2c} (MPa)	109	5	109	10.6	0
F_6 (MPa)	38	4	2	5.7	-26

ing the self healing system to act. Finally, healing tests allowed for 48 Hr of healing time after each cycle, prior to reloading. For most of the data, the coefficient of variation (COV) is in the range 5-15% (Tables 1-2).

The standard test method ASTM D3039⁴⁸ is used to determine E_1 , E_2 , ν_{12} , F_{1r} , and F_{2r} . The standard test method SACMA-SRM-1R-94⁴⁹ is used to determine F_{1c} and F_{2c} . The standard test method ASTM D5379⁵⁰ is used to determine G_{12} and F_6 .

The configuration of ASTM D5379⁵⁰ is used to perform cyclic shear stress-strain tests to obtain the non-linear damaging behavior $\sigma_6(\gamma_6)$ as shown in Figure 1. The loading modulus is measured within a range of strain specified by the standard. The unloading modulus is measured over the entire unloading portion of the data, as shown in Figure 2.

Unrecoverable (plastic) strain can be observed upon unloading, but only after a threshold value of stress (i.e., the yield strength) or strain (i.e., the yield strain) is reached during loading (Figure 3).

Even though plastic strain is accumulated, initially the unloading modulus remain unchanged and equal to the loading modulus. For the unloading modulus to change, that is to decrease below the value of the initial loading modulus, damage must appear. Note that the word "unloading" is added for emphasis and because the reduction in modulus is first detected during unloading of the specimen. But of course the modulus reduction is permanent. A reduction of the unloading modulus with respect to the initial loading modulus can be observed only after a threshold value of stress (i.e., the damage threshold stress) or strain (i.e., the damage threshold strain) is reached during loading (Figure 4).

The threshold stress F_{6EP} for appearance of unrecoverable (plastic) strain (i.e., the yield strength), and the threshold stress F_{6ED} for appearance of irreversible damage, are read from the loading portion of the $\sigma_6(\gamma_6)$ curve (Figure 1) with the aid of Figures 3 and 4.

The unrecoverable (plastic) strain γ_6^p as a function of the applied total strain γ_6 are read for each cycle after full unloading (Figure 2) and reported in Figure 3.

The slope of the unloading curves (Figure 2) provides the damaged elastic modulus G_{12}^d as a function of total applied strain γ_6 (Figure 4).

The amount of damage d at the apex of each cycle (Figure 1) can be computed using the damage model equation

$$G_{12}^d = \bar{G}_{12}(1-d) \quad [1]$$

in terms of the unloading modulus G_{12}^d and the initial (undamaged) modulus \bar{G}_{12} as

$$d = 1 - G_{12}^d / \bar{G}_{12} \quad [2]$$

Upon unloading, the subsequent loading modulus is equal to the last unloading modulus provided there is no healing. The modulus can be partially or totally recovered if the materials is allowed to heal. The amount of healing is represented by h and the damage is reduced, or healed, to a

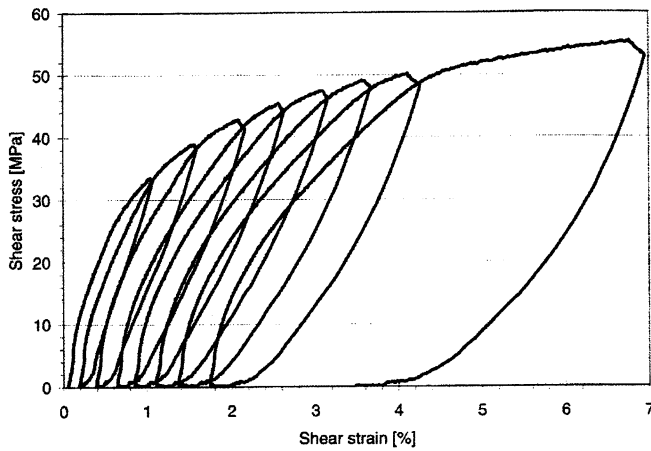


Figure 1. Shear stress-strain behavior of unidirectional, neat specimen (no self-healing system). Loss of stiffness and accumulation of plastic strain are evident.

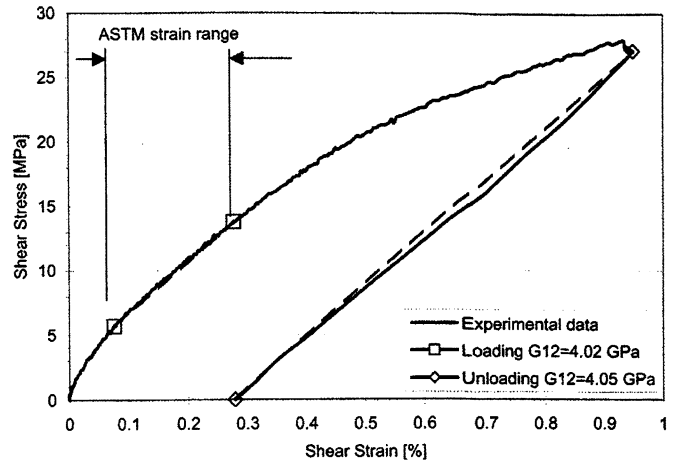


Figure 2. Determination of loading and unloading shear modulus of unidirectional sample as per ASTM D5379.

new value

$$d_h = d - h \quad [3]$$

The loading modulus is then

$$G_{12}^{d_h} = \bar{G}_{12}(1 - d_h) \quad [4]$$

A definition for the efficiency η^d of the healing system is proposed as

$$\eta^d = \frac{G_{12}^{d_h} - G_{12}^d}{\bar{G}_{12} - G_{12}^d} \quad [5]$$

in terms of the initial (virgin) shear modulus \bar{G}_{12} , damaged (unloading) shear modulus G_{12}^d , and healed (loading) shear modulus $G_{12}^{d_h}$, which are all measurable parameters.

The parameters G_{23} , v_{23} , F_4 , and G_{23}^d , were not measured in this investigation because we focused on in-plane behavior only.

The evolution of plastic strain is modeled with

$$\gamma_6^p = a_1^p(\gamma_6 - \gamma_6^{0p}) + a_2^p(\gamma_6 - \gamma_6^{0p})^2 \quad [6]$$

where a_1^p , a_2^p , γ_6^{0p} are adjusted to fit the experi-

mental data as shown in Figure 3, with γ_6^{0p} being the yield strain.

The reduction of shear modulus is modeled with the linear relationship

$$(G_{12}^d - \bar{G}_{12}) = a_1^d(\gamma_6 - \gamma_6^{0d}) \quad [7]$$

where a_1^d and γ_6^{0d} are adjusted to fit the experimental data as shown in Figure 4, with γ_6^{0d} being the damage threshold strain.

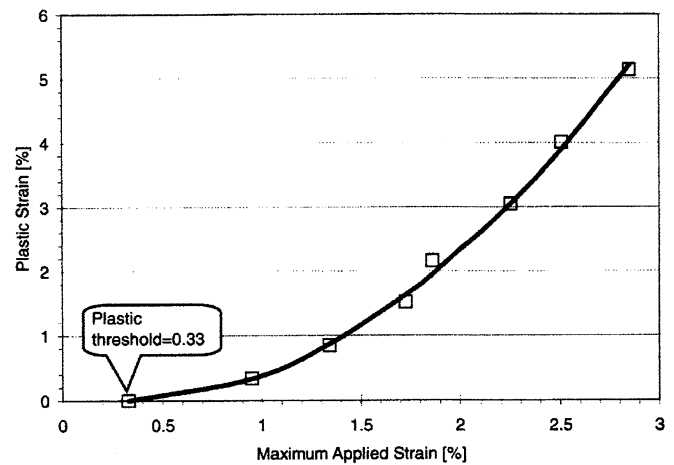


Figure 3. Plastic strain vs. applied strain for unidirectional, neat specimen (no self-healing system). Threshold plastic strain (i.e., yield strain) is evident.

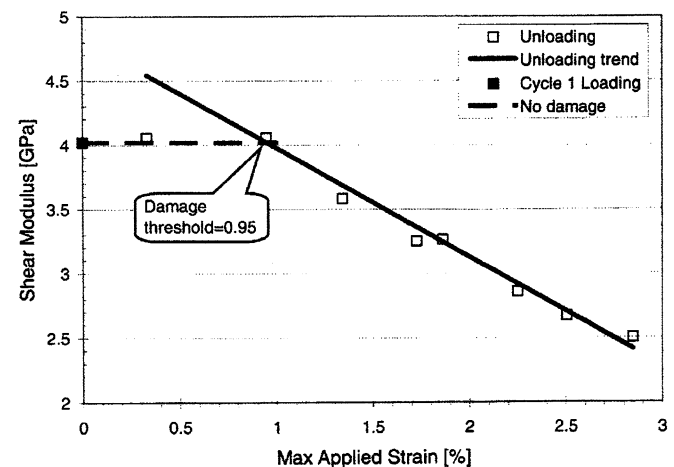


Figure 4. Shear modulus vs. applied strain of unidirectional, neat specimen (no self-healing system). Threshold damage strain is evident.

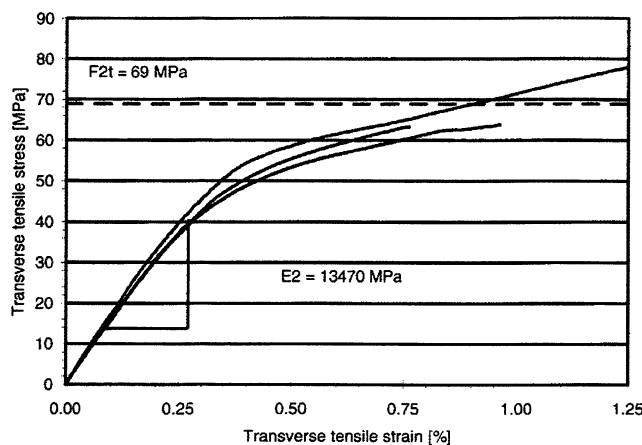


Figure 5. Transverse tensile stress-strain behavior of three unidirectional, neat specimens (no self-healing system). Loss of stiffness is evident.

Effect on Initial Properties

The self healing system occupies space that otherwise could be occupied by neat resin, which results in reduction of longitudinal, transverse, and shear stiffness. Material properties are reported in Table 1 for the unidirectional composite without self-healing system and in Table 2 for the composite with the self-healing system but not allowed to heal. Addition of micro-capsules results in a reduction of the longitudinal compressive strength but not of transverse compression strength. Furthermore, longitudinal tensile, transverse tensile, and shear strength are reduced due to the presence of the micro-capsules. On the other hand, dispersion of micro-capsules has a beneficial effect on fracture toughness, as reported in³⁰.

It can be seen in Table 2 that most properties are significantly degraded by the inclusion of the self-healing system. It must be noted that in this study the %wt of micro-capsules and encapsulated catalyst were purposely set to high values in order to obtain noticeable and significant effects of healing on the observed behavior. It remains for a subsequent study to optimize the tradeoff between knock-down of initial properties and self-healing recovery.

Damage Effects

It is important to note that continuum damage mechanics (CDM), and by extension continuum damage-healing mechanics (CDHM⁴⁰), does not attempt to identify the precise damage mechanisms that take place. Instead, damage is just a state variable that represents the loss of stiffness due to damage⁵¹. In this manuscript, healing is simply damage recovery, which is equivalent to stiffness recovery⁴⁰.

Loss of stiffness due to damage is evident in all tensile and shear tests of unidirectional samples with or without embedded self healing, but it is more evident for transverse tensile (Figure 5) and shear loading (Figure 4). The loss of stiffness during transverse tensile tests is shown in Figure 5 for the sample without self-healing system. Simi-

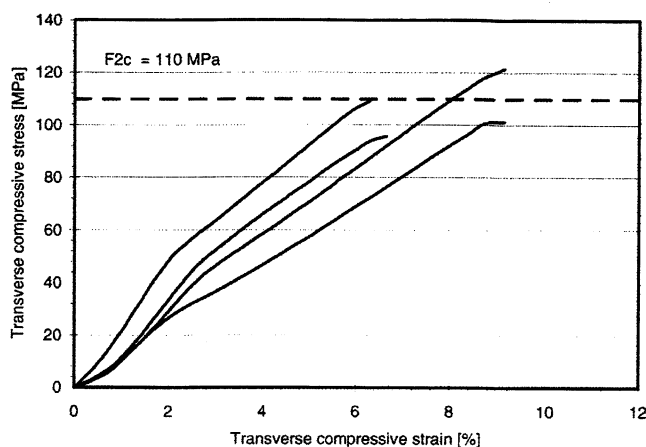


Figure 6. Transverse compression stress-strain behavior of four unidirectional samples with self-healing system. Note the early loss of stiffness.

lar behavior is observed in the samples with self-healing system.

Transverse compression tests of unidirectional samples with self healing system show noticeable but not severe loss of stiffness at about one-third of the transverse compression strength (Figure 6).

Existence of damage and a damage threshold are demonstrated by the fact that measured unloading modulus is less than the loading modulus after the damage threshold has been reached (Figure 4). No loss of stiffness occurs when the applied strain is less than the threshold. After the threshold is reached, the loss of modulus is proportional to the applied strain. Since careful visual inspection after each loading cycle does not reveal appearance of any macro-crack, the loss of modulus is attributed and modeled as distributed damage.

Also noticeable in Figure 3 is the accumulation of unrecoverable (plastic) strain. While the physical, microstructural, and morphological mechanisms leading to plasticity in polymers are different than those leading to plasticity in metals, from a phenomenological and modeling point of view, unrecoverable deformations can be modeled with plasticity theory as long as the plastic strains are not associated to a reduction of the unloading modulus. The reduction of unloading modulus, which occurs independently of the plastic strain, can be accounted for by continuum damage mechanics. Each of these two phenomena have different thresholds for initiation and evolve with different rates. They are, however, coupled by the redistribution of stress that both phenomena induce. In the model this is taken into account by formulating the plasticity model in terms of effective stress computed by the damage model⁴⁰.

Shear tests reveal marked non-linearity (Figure 1) reaching almost total loss of tangent stiffness prior to failure, which occurs at large values of shear strain. Unloading secant stiffness reveals marked loss of stiffness due to damage, which worsens during cyclic re-loading (Figure 4). Also, unloading reveals significant plastic strains, ac-

cumulating during cyclic re-loading (Figure 3). These effects are observed for both types of samples, with and without embedded self healing.

The unidirectional material without healing system has a plastic threshold $\gamma_6^{0p}=0.33\%$, which is lower than the damage threshold $\gamma_6^{0d}=0.95\%$. At first, the material accumu-

lates plastic strain without noticeable loss of unloading modulus. A typical loading-unloading cycle is depicted in Figure 2.

Healing Effects

When the material is allowed to heal for 48 Hr after each load-unload cycle, marked recovery of shear stiffness is observed in subsequent shear loading (Figure 7). Repeated loading-unloading-healing cycles reveal that the healing system is eventually exhausted. Although the healing process only delays the final outcome, such delay might be crucial to maintain the integrity and/or operational capability of in-service components. In other words, self-healing provides artificial toughening to an otherwise brittle system.

Since all the cycles depicted in Figure 8 were loaded to approximately the same strain (about 2.5%), the plastic strain does not increase with the number of cycles. Also, the plastic strain is not affected by healing, thus providing further evidence that the plasticity phenomena is independent of the damage-healing phenomena.

In Figure 8, all the damage introduced in the first two loading cycles is completely healed with 100% healing efficiency. After that, the healing action is unable to fully recover the initial modulus. In other words, after the second cycle, not all of the damage can be healed. However, healing effects are still noticeable after eight cycles at 2.5% strain each.

Twenty-two unidirectional samples containing self-healing system were loaded in shear with one and one-half

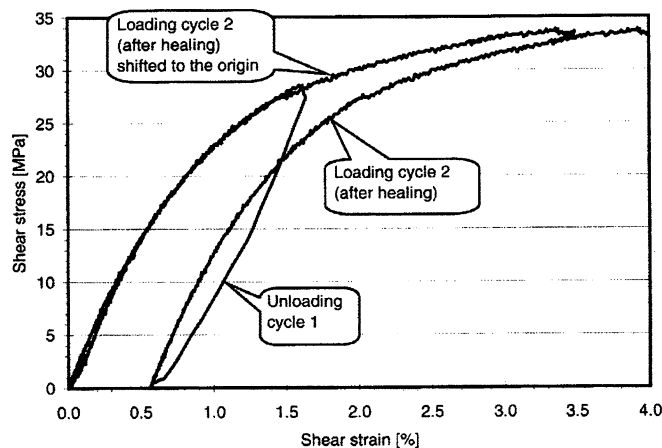


Figure 7. Unidirectional composite specimen allowed to heal for 48 hr. The modulus is recovered with efficiency 0.983.

cycles consisting of loading, unloading, followed by 48 Hr of healing time, and then re-loaded. Each specimen was loaded to a unique value of maximum applied shear strain in the range 0.5 to 4.0% strain with roughly equal number of specimens loaded up to 0.5, 1.0, ..., 4.0% strain at intervals of 0.5%. A yield strain threshold value is apparent in Figure 9.

Damage is calculated using Equation 2 and measured values of loading and unloading shear moduli. Healing efficiency is calculated using Equation 5 and measured values of initial, damaged, and healed shear moduli. A clear value of yield strain can be obtained from the intercept in Figure 9, where linear accumulation of plastic strain is clearly observed.

Conclusions

This paper summarizes the previous work done in the field of self-healing composite materials, which considered healing of macro-cracks, and presents new results with a similar system where micro-cracks are healed. The healing is quantified using a continuum damage mechanics approach by evaluating the residual stiffness of the composite after load induced damage. The proposed healing efficiency (Equation 5) is a novel contribution to the field of self-healing. A methodology is presented that can be used to characterize damage and healing of distributed micro-cracking damage. Efficiencies of up to 1.0 were easily obtained, even after two loading cycles, thus demonstrating successful fabrication that maintained the integrity of the encapsulated healing agent while allowing release of the healing agent under the action of distributed micro-crack damage. Knockdown of nominal properties due to the inclusion of the self-healing system were found to be significant. The existence of a yield strain and a damage threshold is demonstrated both by repeated cyclic loading-unloading of individual specimens and by single-cycle experiments on a large sample population loaded to various values of strain within a large range of strain.

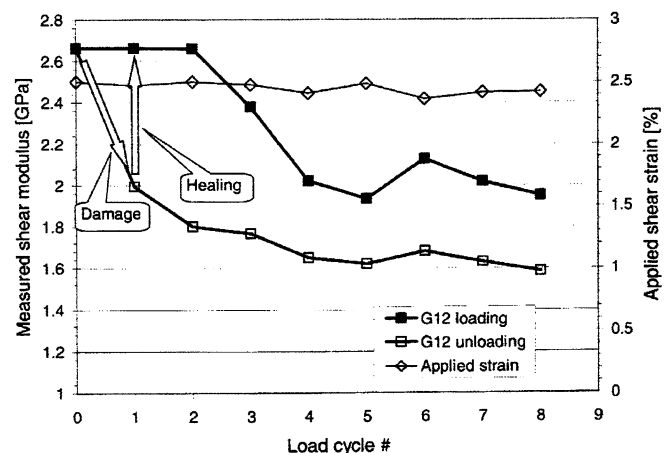


Figure 8. Unidirectional composite specimen loaded to 2.5% strain, unloaded, and allowed to heal for 48 hr. The cycle is repeated several times.

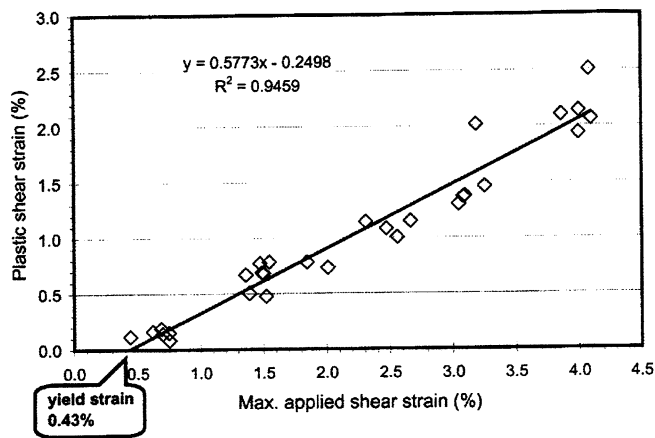


Figure 9. Plastic strain vs. applied strain for several unidirectional composite specimens, each loaded with a single-cycle.

Acknowledgements

The authors wish to acknowledge Chuck Coleman and Cliff Judy for their help with instrumentation and machining, Dr. Peter Stansberry for allowing us to use his lab to fabricate micro-capsules, Dr. Alfred Stiller for invaluable insight into microencapsulation methods, and Mark Kozlowski and Raymond Claus for helping in fabricating and testing specimens.

References

1. E.J. Barbero, Introduction to Composite Materials Design, *Taylor and Francis*, Philadelphia, 1999.
2. R. Verberg, A.T. Dale, P. Kumar, A. Alexeev, A.C. Balazs, Healing Substrates with Mobile, Particle-filled Microcapsules: Designing a 'Repair and Go' System, *J. of the Royal Society*.
3. K.A. Williams, A.J. Boydston, C.W. Bielawski, Towards Electrically Conductive, Self-healing Materials, *J. of the Royal Society*.
4. R.S. Trask, G.J. Williams, I.P. Bond, Bioinspired Self-healing of Advanced Composite Structures using Hollow Glass Fibres, *J. of the Royal Society*.
5. F.R. Kersey, D.M. Loveless, S.L. Craig, A Hybrid Polymer Gel with Controlled Rates of Cross-link Rupture and Self-repair, *J. of the Royal Society*.
6. S.J. Kalista, T.C. Ward, Thermal Characteristics of the Self-healing Response in Poly(ethylene-co-methacrylic acid) Copolymers, *J. of the Royal Society*.
7. S. White, N. Sottos, P. Guebelle, J. Moore, M. Kessler, S. Sriram, E. Brown, S. Viswanathan, Autonomic Healing of Polymer Composites, *Nature* 409 (6822) (2001) 794-7.
8. S. White, N. Sottos, P. Geubelle, J. Moore, M. Kessler, S. Sriram, E. Brown, S. Viswanathan, Erratum: Autonomic Healing of Polymer Composites (*Nature* (2001) 409 (794-797)), *Nature* 415 (6873) (2002) 817.
9. N. Sottos, S. White, I. Bond, Introduction: Self-healing Polymers and Composites, *J. of the Royal Society*.
10. T.C. Mauldin, J.D. Rule, N.R. Sottos, S.R. White, J.S. Moore, Self-healing Kinetics and the Stereoisomers of Dicyclopentadiene, *J. of the Royal Society*.
11. E. Brown, N. Sottos, S. White, Fracture Testing of a Self-healing Polymer Composite, *Experimental Mechanics* 42 (4) (2002) 372-9.
12. M. Kessler, S. White, Self-activated Healing of Delamination Damage in Woven Composites, *Composites - Part A: Applied Science and Manufacturing* 32 (5) (2001) 683-699.
13. S.A. Hayes, W. Zhang, M. Branthwaite, F.R. Jones, Self-healing of Damage in Fibre-reinforced Polymer-matrix Composites, *J. of the Royal Society*.
14. A.S. Jones, J.D. Rule, J.S. Moore, N.R. Sottos, S. R. White, Life Extension of Self-healing Polymers with Rapidly Growing Fatigue Cracks, *J. of the Royal Society*.
15. M. Kessler, N. Sottos, S. White, Self-healing Structural Composite Materials, *Composites Part A: Applied Science and Manufacturing* 34 (8) (2003) 743-753.
16. M. Kessler, S. White, Cure Kinetics of the Ring-opening Metathesis Polymerization of Dicyclopentadiene, *Journal of Polymer Science, Part A: Polymer Chemistry* 40 (14) (2002) 2373-2383.
17. J.D. Rule, J.S. Moore, Romp Reactivity of Endo- and Exo-dicyclopentadiene, *Macromolecules* 35 (21) (2002) 7878-7882.
18. P. Schwab, R.H. Grubbs, J.H. Ziller, Synthesis and Applications of $\text{RuCl}_2(\text{=CHR})(\text{PR}_3)_2$: The influence of the Alkylidene Moiety on Metathesis Activity, *Journal of the American Chemical Society* 118 (1) (1996) 100-.
19. S. Alexandridou, C. Kiparissides, J. Fransaeer, J. Celis, On the Synthesis of Oil-containing Microcapsules and Their Electrolytic Codeposition, *Surface & Coatings Technology* 71 (3) (1995) 267-276.
20. R. Arshady, Polymerization in Dispersed Systems: Methodology and Terminology, In: *American Chemical Society, Polymer Preprints, Division of Polymer Chemistry, Vol. 38, ACS, Washington, DC, USA, Las Vegas, NV, USA, 1997*, pp. 636-637.
21. R. Arshady, M.H. George, Suspension, Dispersion, and Interfacial Polycondensation, A Methodological Survey, *Polymer Engineering and Science* 33 (14) (1993) 865-876.
22. G. Baxter, Microencapsulation Technology and Modern Business Forms., *Tappi* 60 (5) (1977) 84-86.
23. M.R. Kessler, Characterization and Performance of a Self-healing Composite Material, Ph.D. thesis, University of Illinois Urbana Champaign, IL (2002).
24. B. Ovez, B. Citak, D. Oztemel, A. Balbas, S. Peker, S. Cakir, Variation of Droplet Sizes During the Formation of Microspheres from Emulsions, *Journal of Microencapsulation* 14 (1997) 489-499.

25. H.S. Tan, T.H. Ng, H.K. Mahabadi, Interfacial Polymerization Encapsulation of a Viscous Pigment Mix - Emulsification Conditions and Particle-size Distribution, *Journal of Microencapsulation* 8 (1991) 525-536.
26. C. Thies, *Encyclopedia of Polymer Science and Engineering*, Vol. 9, 2nd Ed., Wiley, 1987, Ch. Microencapsulation.
27. N. Yan, P. Ni, M. Zhang, Preparation and Properties of Polyurea Microcapsules with Nonionic Surfactant as Emulsifier, *Journal of Microencapsulation* 10 (1993) 375-383.
28. E.N. Brown, M.R. Kessler, N.R. Sottos, S.R. White, In Situ Poly(urea-formaldehyde) Microencapsulation of Dicyclopentadiene, *Journal of Microencapsulation*.
29. R. Wool, K. O'Connor, A Theory of Crack Healing in Polymers, *Journal of Applied Physics* 52 (10) (1981) 5953-63.
30. E. Brown, S. White, N. Sottos, Microcapsule Induced Toughening in a Self-healing Polymer Composite, *Journal of Materials Science* 39 (5) (2004) 1703-10.
31. J.D. Rule, E.N. Brown, N.R. Sottos, S.R. White, J.S. Moore, Wax-protected Catalyst Microspheres for Efficient Self-healing Materials, *Advanced Materials* 17 (2) (2005) 205-208.
32. S. Miao, M.L. Wang, H.L. Schreyer, Constitutive Models for Healing of Materials with Application to Compaction of Crushed Rock Salt, *Journal of Engineering Mechanics* 121 (10) (1995) 1122-1129.
33. S. Jacobsen, J. Marchand, L. Boisvert, Effect of Cracking and Healing on Chloride Transport in OPC Concrete, *Cement and Concrete Research* 26 (6) (1996) 869-881.
34. S. Jacobsen, E.J. Sellevold, Self Healing of High Strength Concrete after Deterioration by Freeze/Thaw, *Cement and Concrete Research* 26 (1) (1996) 55-62.
35. W. Nakao, S. Mori, J. Nakamura, K. Takahashi, K. Ando, M. Yokouchi, Self-crack-healing Behavior of Mullite/SiC Particle/SiC Whisker Multi-composites and Potential use for Ceramic Springs, *Journal of the American Ceramic Society* 89 (4) (2006) 1352-1357.
36. K. Ando, K. Furusawa, K. Takahashi, S. Sato, Crack-healing Ability of Structural Ceramics and a New Methodology to Guarantee the Structural Integrity using the Ability and Proof-test, *Journal of the European Ceramic Society* 25 (5) (2005) 549-58.
37. J. Adam, A Mathematical Model of Wound Healing in Bone, in: *Proceedings of the International Conference on Mathematics and Engineering Techniques in Medicine and Biological Sciences. METMBS'00*, Vol. 1, CSREA Press - Univ. Georgia, Las Vegas, NV, 2000, pp. 97-103.
38. J. Adam, A Simplified Model of Wound Healing (with Particular Reference to the Critical Size Defect), *Mathematical and Computer Modelling* 30(5-6)September (1999) 23-32.
39. A. Simpson, T.N. Gardner, M. Evans, J. Kenwright, Stiffness, Strength and Healing Assessment in Different Bone Fractures - A Simple Mathematical Model, *Injury* 31(10, December) (2000) 777 - 781.
40. E.J. Barbero, F. Greco, P. Lonetti, Continuum Damage-healing Mechanics with Application to Self-healing Composites, *International Journal of Damage Mechanics* 14 (1) (2005) 51-81.
41. E.J. Barbero, L. De Vivo, Constitutive Model for Elastic Damage in Fiber-reinforced PMC Laminae, *International Journal of Damage Mechanics* 10 (1) (2001) 73-93.
42. E.J. Barbero, P. Lonetti, Damage Model for Composites Defined in Terms of Available Data, *Mechanics of Composite Materials and Structures* 8 (4) (2001) 299-315.
43. E.J. Barbero, P. Lonetti, An Inelastic Damage Model for Fiber Reinforced Laminates, *Journal of Composite Materials* 36 (8) (2002) 941-962.
44. P. Lonetti, R. Zinno, F. Greco, E. J. Barbero, Interlaminar Damage Model for Polymer Matrix Composites, *Journal of Composite Materials* 37 (16) (2003) 1485-1504.
45. P. Lonetti, E.J. Barbero, R. Zinno, F. Greco, Erratum: Interlaminar Damage Model for Polymer Matrix Composites (*Journal of Composite Materials* 37: 16 (1485-1504)), *Journal of Composite Materials* 38 (9) (2004) 799-800.
46. E. Barbero, P. Lonetti, K. Sikkil, Finite Element Continuum Damage Modeling of Plain Weave Reinforced Composites, *Composites Part B: Engineering* 37 (2-3) (2006) 137-147.
47. E.J. Barbero, Self-healing Materials, Wiley, 2007, Ch. Modeling of Self-healing Mechanics.
48. ASTM, D3039 Standard Test Method for Tensile Properties of Polymer Matrix Composite Materials, ASTM 15.03.
49. SACMA, SACMA srm 1r-94, SACMA Recommended Test Method for Compressive Properties of Oriented Fiber-resin Composites, Suppliers of Advanced Composite Materials Association, Arlington, VA 22209. 1R.
50. ASTM, D5379 Standard Test Method for Shear Properties of Composite Materials by the V-notched Beam Method, ASTM 15.03.
51. J. Lemaitre, J.-L. Chaboche, Phenomenological Approach of Damage Rupture, *Journal de Mecanique Appliquee* 2 (3) (1978) 317-65.